U.P.B. Sci. Bull., Series A, Vol. 86, Iss. 1, 2024 ISSN 1223-7027

APPLICATION OF SPECTROSCOPIC AND DIFFRACTION METHODS FOR PHOTOCATALYTIC INVESTIGATION OF SYNTHETIC CLAYS

Kahina BENTALEB[1], Abdulrahman AL AMERI[1,2], Zohra BOUBERKA[1,2], Zohra TAIBI[1], Ana BARRERA[2], Rachida Khadidja BENMAMMAR[2], Ulrich MASCHKE[2]

In this work, the photocatalytic efficiency of TiO_2 was improved by its immobilization. Synthetic clays (Layered Double Hydroxides or LDHs) were chosen as support since LDHs allow for easier recovery of TiO_2. The characterization of the TiO_2/LDH composite by infrared spectroscopy, chemical analysis, and X-ray diffraction confirmed the fixation of TiO_2 on LDH. The depollution study focused particularly on Trichlorophenol as a model pollutant, by varying different physico-chemical parameters. This work brings together both the results of the characterization of the TiO_2/LDH material used, and the results obtained following the photodegradation of trichlorophenol by the latter.

Keywords: X-Ray diffraction; Fourier Transform Infrared Spectroscopy; Atomic emission spectroscopy; Photocatalysis; Layered Double Hydroxides.

1. Introduction

Environmental pollution, especially water pollution by organic compounds, has become a major global concern and has attracted the attention of scientists worldwide. Aromatic compounds in general, and phenols in particular, with their certain toxicity, are now considered carcinogenic and hazardous organic micropollutants, even when present in trace amounts. They typically originate from the manufacture of products such as cresol-based resins, herbicides, pharmaceuticals, and surfactants, which often end up in industrial wastewater. Most of these compounds are persistent organic pollutants due to their resistance to conventional chemical, biological and photolytic processes. This poses a serious health problem, mainly due to their toxicity and potentially dangerous health effects (carcinogenicity, mutagenicity, and bactericidal effects) on living organisms, including humans [1]. Chlorophenols (CPs) are a group of organic

[1] Laboratoire Physico-Chimie des Matériaux-Catalyse et Environnement (LPCMCE), Université des Sciences et de la Technologie d'Oran Mohamed Boudiaf (USTOMB), BP 1505, El M'naouer, 31000 Oran, Algeria
[2] Unité Matériaux et Transformations (UMET), UMR 8207, Université de Lille, CNRS, INRAE, Centrale Lille, F-59000 Lille, France, e-mail: ulrich.maschke@univ-lille.fr

substances introduced into the environment as a result of various man-made activities, such as water disinfection, waste incineration, uncontrolled pesticides, and herbicides, etc., as well as by-products of chlorine bleaching of pulp. Due to their multiple sources, they can be found in industrial effluents, soils, and surface waters, and several of them have been listed among the 65 priority pollutants by the US EPA [2]. Phenolic compounds, a class of aromatic hydrocarbon derivatives, are widely used as active ingredients in herbicides, insecticides, pharmaceuticals, dyes, as well as preservatives in wood processing in various industrial sectors [3]. The discharge of wastewater containing CPs into natural water bodies can cause serious environmental and ecotoxicological problems, as many of them are suspected to be carcinogenic and mutagenic [4].

Therefore, several degradation pathways are possible for these pollutants. Conventionally applied treatments are based on physical mass transfer methods (sedimentation, filtration, adsorption), or chemical methods (chemical oxidation with ozone, chlorine), or biological methods [5-7]. Although biological treatments are widely used, they remain ineffective against certain toxic and recalcitrant compounds, since they simply transfer contaminants from one phase to another without destroying them [8].

In recent years, much of the work published in the literature has focused on the emergence of new treatment processes, among which Advanced Oxidation Processes (AOPs) occupy an important place [9]. The decomposition or chemical dissociation induced by exposure to visible or ultraviolet light is considered a particularly promising technique [10]. Significant developments have shown great efficiency in decontaminating wastewater contaminated with toxic and persistent pesticides, synthetic organic dyes, pharmaceuticals, personal care products, and a large number of industrial pollutants [11]. AOPs include several techniques such as ozonation, ultraviolet (UV)/O_3, UV/H_2O_2, electro-Fenton, plasma processes, and photocatalysis [12-19]. Photocatalysis is a suitable method for removing toxic substances from water due to its ease of use, reliability, non-toxicity, cost effectiveness, and minimal secondary pollution and thorough mineralization [1,20]. In general, inorganic semiconductors are used as photocatalysts, with titanium dioxide (TiO_2) being the most studied due to its natural abundance, low cost, and stability during photocatalysis [21,22]. Studies have shown that most organic pollutants can be completely eliminated by photocatalysis. However, photocatalysis cannot be used as a single water treatment process, due to the strong hydrophilicity of nano-TiO_2, which prevents hydrophobic organic pollutants from reaching its surface, which is necessary for their photodegradation.

To be effective on an economically viable scale, it must be combined with adsorption, due to its simplicity and high efficiency, as well as the availability of a wide range of adsorbents. For this, supports for TiO_2 nanoparticles such as montmorillonite [23-25], zeolites [26-28] and carbon nanomaterials [29-31] have been effectively used to enhance the photocatalytic activity. An et al. [32] showed that TiO_2 deposited on organophilic montmorillonite completely degraded decabromodiphenyl ether. Gómez-Solís et al. [33] found that SiC (silicon carbide)-TiO_2 catalyst had higher photocatalytic activity toward organic dyes than TiO_2. Huang et al. [34] deposited nano-TiO_2 on hydrophobic hydroxides (LDH) to effectively remove dimethylphthalate from water. A layered hydroxide (LDH) is a hydroxide composed of two or more metal cations with a layered brucite-type crystalline structure. Several methods have been developed for the synthesis of LDH, such as the direct coprecipitation [35], the urea method [36], the anion exchange [37] and the reconstruction methods [38,39]. Coprecipitation is the most widely used synthesis method, which allows obtaining LDHs with a wide variety of cations and anions in the sheets and inter-sheets [40]. In general, the total concentrations of CPs in surface waters range from 0.005 to 20 μg/L. However, the concentrations of CPs in wastewater and in some polluted surface waters can reach up to 1000 μg/L [41]. CPs are polar compounds, and their polarity decreases with increasing number of chlorine substitutions on the benzene ring [42,43]. They are mainly released in waste water generated by petrochemical industries, olive oil production and various chemical manufacturing industries such as those that produce phenolic resins, solvents, paints, plastics and other chemicals [44,45]. They are used in the production of disinfectants, germicides, precursors of pesticides and dyes, in the wood industry as preservatives, in the paper industry, in cosmetics, and in oil refining [46].

The aim of this work is to contribute to the field of elaboration, characterization of new material type LDHs and their application for wastewater treatment, highlighting the synthesis of LDH by co-precipitation in the presence of TiO_2 particles. The 2,4,6-trichlorophenol (TCP) is chosen as a model compound in this study because of its mutagenicity and carcinogenicity. TCP represents a resistant organochlorine compound in aqueous systems and it is necessary to convert it into harmless species [47,48].

2. Experimental

2.1. Materials

All solutions were prepared using high purity distilled water. Potassium hydroxide (KOH, Sodium hydroxide (NaOH), Hydrochloric acid (HCl), Titanium tetrachloride ($TiCl_4$) (Aldrich, 99%), Metal chloride ($MgCl_2$ $6H_2O$ and $AlCl_3$ $6H_2O$) were obtained from Sigma Aldrich (Saint Quentin Fallavier, France).

TCP is presented as yellow flakes with a strong phenolic odor, practically soluble in water at 0.8 g/L, which was obtained from Aldrich (purity 98%). The

UV-spectrum shows characteristic bands at λ values of 205 and 290 nm, proving the presence of benzene rings and phenolic bonds, respectively (Fig. 1).

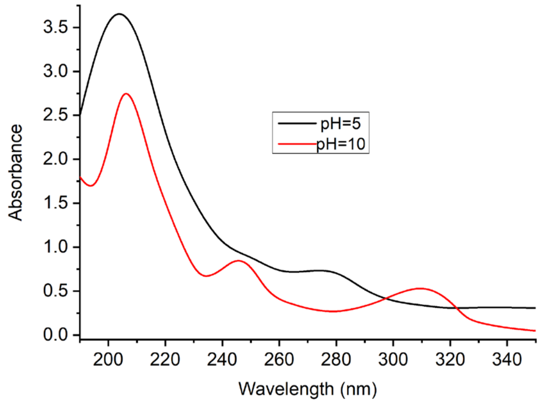

Fig. 1. UV-visible spectrum of 2-4-6-trichlorophenol (TCP) at different pH (5 and 10)

Of particular importance is that TCP has a much lower pKa value (about 6.15 [49]) compared to mono- and di-chlorophenols, indicating that it is widely deprotonated in wastewater and natural waters (usually where pH > 7) [50]. There are two types of TCP species present in natural aquatic environments: non-ionized phenol and ionized phenolate anion [51]. A bathochromic effect is observed with a hyperchromic effect at 210 and 310 nm (Fig. 1).

2.2. Colloid synthesis

$TiCl_4$ colloids were prepared from the hydrolysis of $TiCl_4$; where the amount of 16 mL of distilled water was introduced into an Erlenmeyer flask, then 8 mL of pure $TiCl_4$ was added dropwise under vigorous stirring, at a temperature of about 1°C, resulting in the following chemical reaction:

$$TiCl_4 + 2H_2O \rightarrow TiO_2 + 4HCl$$

The solution was then stirred for 30 min with less vigorous stirring. A transparent yellow solution of $TiCl_4$ is obtained. In order to increase the pH of the colloidal solution of $TiCl_4$ which was initially very acidic, a jump in pH was realized using a KOH solution (2N). An ultrasonic wave irradiation device was used at 9500 rpm.

2.3. Synthesis of composites by coprecipitation at constant pH

The TiO_2/LDH composites were prepared by dropwise addition of a mixed salt solution (Mg^{2+}, Al^{3+}) in a vessel containing TiO_2 (the stoichiometric ratio was 2) to maintain a constant pH value during precipitation. At the end of the synthesis, the reaction product was recovered by centrifugation, then washed and dried at 60°C.

2.4. Analysis methods

X-ray Diffraction analysis [52-55] was performed on a Siemens D5000 automatic powder diffractometer using the Cu Kα line of wavelength λ=1.54056 Å. The rotation speed was 0.01°/s with a step of 0.02°. The spectra were recorded for angles 2θ from 2 to 40°. The mean size of the crystalline domains (D) was calculated using the Scherrer formula [52]

$$D = K\,\lambda / \beta \cos\theta \tag{1}$$

where K represents a dimensionless shape factor with a typical value of 0.9, β stands for the width measured at half the height of the diffraction peak (measured in radians), and θ refers to the Bragg angle.

Fourier-Transform Infrared spectroscopy (FTIR) spectra [56,57] were obtained using a Bruker IKFS 240 spectrometer in the range of 400 to 4000 cm^{-1}. The samples were prepared as a dispersion of clay in an KBr pellet (1/200 by weight).

During photocatalysis [58], the irradiated solution was placed in a reflective enclosure and continuously stirred with a mechanical stirrer. The starting pollutant TCP as well as the degraded samples were analyzed by UV-Vis spectrophotometry to monitor the evolution of degradation using a double beam SAFAS instrument. The spectra were recorded between 190 and 400 nm with steps of 5 nm. The analysis were carried out in 10 mm Quartz cuvettes.

2.5. Photodegradation procedure

The photocatalytic degradation of TCP with the TiO_2/LDH nanocomposite material was carried out by UV light in a photocatalytic oxidation reactor, consisting of three 6 W UV fluorescent black light lamps (λmax=365 nm) used as artificial light sources. A cylindrical Pyrex jacket was used as a reactor around the cover tube, containing a water-cooling circuit to absorb the IR radiation and thus avoid heating of the solution. Constant stirring of the solution was maintained by a magnetic stirrer.

All photodegradation experiments were performed with the same reaction volume of 100 mL, at room temperature. The suspension was first stirred in the dark for 30 min before irradiation, which was sufficient to reach adsorption equilibrium. Irradiation started at time t=0s and samples of the suspensions were taken at regular time intervals, centrifuged, and analyzed.

The degradation spectra of the pollutant in the UV wavelength range were recorded as function of the initial pollutant concentration, pH, and mass of the synthesized material (TiO_2/LDH).

3. Results and discussion

3.1. LDH characterization by plasma atomic emission spectroscopy

Elemental analysis (Mg, Al and Ti) was performed using inductively coupled plasma atomic emission spectroscopy (ICP/AES) [59-61]. In order to study the formation of the LDH phases, the elemental analysis of the different samples (Mg_2-Al) and Mg_2-Al-TiO_2), were determined by ICP-AES and are summarized in Table 1. The analysis was carried out to confirm the TiO_2 content in Mg_2-Al-TiO_2, and to calculate the Mg/Al, Mg/Ti and Al/Ti ratios. The Mg^{2+} and Al^{3+} contents are comparable to those expected, indicating that the synthesis method was successful. In fact, during the synthesis, TiO_2 is added to the solution, which leads to a decrease in the percentages of MgO and Al_2O_3 and an increase in the percentage of TiO_2. The same has been observed for TiO_2/Zn(2)Al-LDH [62]. The chemical compositions and anion exchange capacities (A.E.C.) were determined by elemental analysis and water content obtained by thermogravimetry.

Table 1

Elemental analysis of Mg_2-Al and Mg_2-Al-TiO_2

Samples	Mg_2-Al	Mg_2-Al-TiO_2
MgO (%)	30.59	24.30
Al_2O_3 (%)	19.19	14.87
Ti (%)	0.005	26.67
Total (%)	49.79	65.84
Mg (%)	18.45	14.65
Al (%)	10.06	7.87
Ti (%)	0	15.99
Mg/Al	2.02	2.07
Mg/Ti	0	1.81
Al/Ti	0	0.87
(Mg+Al)/Ti	0	2.68
H_2O (%)	2.98	2.60
Chemical formula	$Mg_{0.68}Al_{0.32}(OH)_2(CO_3)_{0.16}$ 2.98 (H_2O)	$Mg_{0.66}Al_{0.34}(OH)_2(CO_3)_{0.17}$ 2.60 (H_2O)
A.E.C. (meq/100g)	261.42	204.54

3.2. Structural and spectroscopic analysis of LDH

From the XRD patterns (Fig. 2a) of the powdered materials, Mg_2-Al and Mg_2-Al-TiO_2, it was observed that the samples have the typical XRD pattern corresponding to a hydrotalcite structure. Two samples have reflections with sharp and intense lines at low values of 2Θ angle, estimated from the peaks of (003), (006) and (009), and less intense and asymmetric ones (110) and (113) at higher 2Θ angle [63-66]. No crystalline $Mg(OH)_2$ or $Al(OH)_3$ phase was detected. The 2Θ angle of the (003) reflexion, corresponding to the basal spacing of the clays, was 7.95Å for Mg_2-Al and 7.46Å for Mg_2-Al-TiO_2 sample (equation (1) [52]. These values are close to the d-spacing values reported for hydrotacite with carbonate in the interlayer. The (003) and (110) reflections allow the calculation of unit cell parameters, ($c=3\times d_{003}$) and ($a=2\times d_{110}$). The fine and symmetrical morphology of the peaks reflects a good crystallization of the material. It is arranged according to the hexagonal LDH crystal structure with R3m layer; in good agreement with previously reported literature. The comparison of Mg_2-Al-TiO_2 with Mg_2-Al shows the presence of both TiO_2 and LDH compounds. The intensity of the characteristic peaks of the TiO_2/Mg-Al phase was decreased compared to the peaks obtained in the Mg-Al sample. This result is due to the disorder generated by the incorporation of TiO_2 particles into the LDH sheets [34,67]. The same was observed for Hydrotalcite-TiO_2 magnetic iron oxide intercalated with the anionic surfactant dodecylsulfate HT-DS/TiO_2/Fe23 and HT/TiO_2/Fe34.

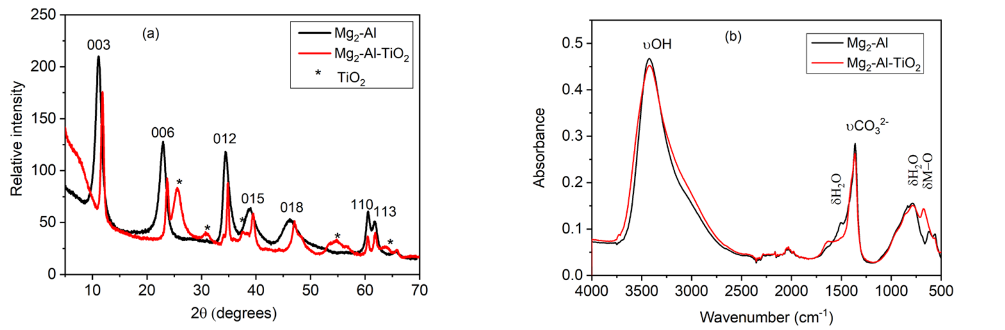

Fig. 2. (a) X-ray diffraction diagrams and (b) ATR-FTIR spectra of Mg_2-Al and Mg_2-Al-TiO_2

The infrared spectra of Mg_2-Al and Mg_2–Al–TiO_2 (Fig. 2b) can be used to identify the structural difference between the different forms of samples. The intense and broad band between 3600 and 3400 cm^{-1} was observed for all samples, corresponding to the stretching vibrations of hydroxyl groups of the sample layers, due to physically adsorbed and intercalated water. Another weak band was found at 1600 cm^{-1}, due to bending vibrations of water molecules. The strong absorption band at 1376 cm^{-1} can be attributed to the stretching vibration of

CO_3. Bands around 700-400 cm^{-1} can be related to the bending vibrations of the metal oxides M-O and O-M-O of the LDH lattice [64,68].

3.3. Surface area of LDH

Fig. 3 shows the nitrogen adsorption-desorption isotherms of Mg_2-Al-TiO_2 and Mg_2-Al. According to the IUPAC classification, both samples exhibited isotherms with a profile similar to that of type IV, with a well-defined H3 hysteresis loop in the mid-range of the relative pressure. The physisorption isotherms of type IV are associated with a capillary condensation occurring in the mesopores, limiting the absorption to a wide range of P/P0, and monolayer–multilayer characteristics of adsorption in the initial part of the isotherm.

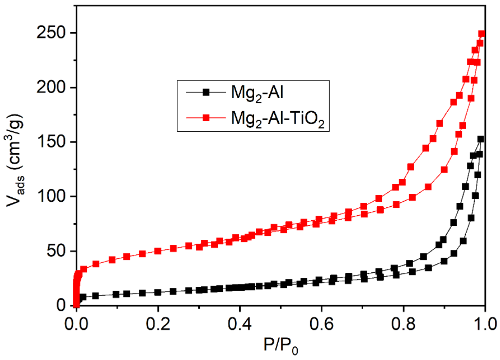

Fig. 3. N_2 adsorption-desorption isotherms of Mg_2-Al and Mg_2-Al-TiO_2

The textural parameters are listed in Table 2. The specific surface areas (SBET) and the total pore volume (VM) increased from 42.33 to 206.71 m²/g and from 0.19 to 0.42 cm^3/g, respectively, while the average pore diameter decreased from 185.59 to 80.87 nm for Mg_2-Al and Mg_2-Al-TiO_2, respectively. The presence of TiO_2 in LDH matrices induces profound changes in the textural properties of the solid, increasing the surface area and pore volume.

Table 2

BET surface area, pore volume and average pore size of Mg_2-Al and Mg_2-Al-TiO_2

Samples	BET area (m²/g)	V_p (cm^3/g)	$\Phi_{average}$ (nm)
Mg_2-Al	42.33	0.19	185.59
Mg_2-Al-TiO_2	206.71	0.42	80.87

3.4. Discussion of the photodegradation process

In the absence of UV light, the removal of TCP by adsorption was evaluated. The Mg_2-Al-TiO_2 photocatalyst adsorbed 3% of the TCP after 200 min in the absence of UV radiation. UV photolysis alone degraded 1% of the initial

TCP. The photoactivity of TiO_2 is mainly concentrated in the UV light region, while the photoactivity of Mg_2-Al-TiO_2 sample shifts to the visible light region. Mg_2-Al-TiO_2 was more photocatalytically active for the degradation of TCP than pure TiO_2 (10%). The synergistic effect was attributed to a higher production of OH radicals formed from the structural hydroxides.

The pH plays an important role in the degradation processes. The effect of pH on the degradation behavior of TCP was studied at pH 3 and 10. The choice of this range was made in order to study the evolution of the degradation of the pollutant associated with the different chemical forms: molecular and ionic at acidic (Fig. 4a) and basic pH (Fig. 4b), respectively. To study this parameter, a concentration of 0.8 mmol/L was used for the two pH values. The characteristic peaks of TCP disappear at basic pH (Fig. 4b), reaching an extent of photocatalytic removal of TCP of 65%. The pH also affects the reaction rate. In the case of TiO_2 as a photo-catalyst, the surface is charged as follows:

$$TiOH + H^+ \leftrightarrow TiOH_2^+ \quad (pzc) < 6.5)$$

$$TiOH \leftrightarrow TiO^- + H^+ \quad (pzc > 6.5)$$

In an acidic medium, the surface is positively charged, while in an alkaline medium, it is negatively charged. For this reason, the following experiments were per-formed at two pH values, one lower and one higher than pzc (point of zero charge). This change in surface charge affects the adsorption of reactive molecules and influences the degradation kinetics.

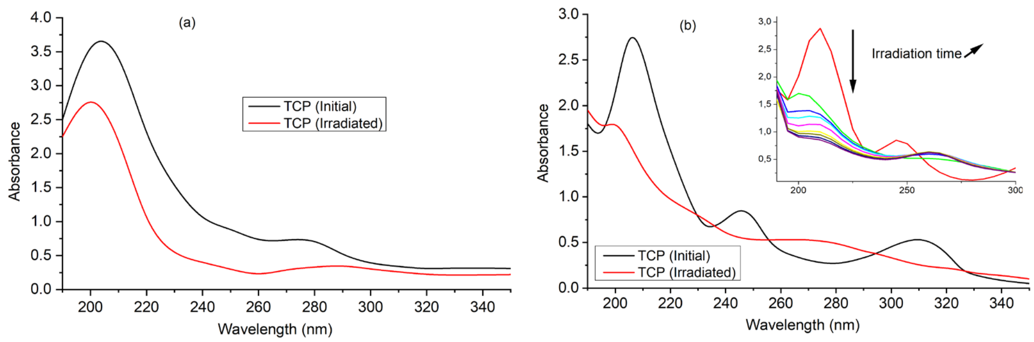

Fig. 4. UV-visible spectra of initial and irradiated TCP at (a) acid pH (pH=3) and (b) basic pH (pH=10)

The results showed that better photodegradation of TCP is achieved at pH=10. Saritha et al. [69] reported that the best degradation of TCP with UV/Fenton is at pH=3. According to Ali et al. [70], it occurred at medium pH values with TiO2@rGO catalyst.

In order to study the influence of the initial concentration of TCP on the synthesized LDH and the effect of the TCP concentration on its degradation, three concentrations in the range of 0.5 to 1 mM were selected by adding an amount of 0.1 g of TiO_2-LDH in a volume of 100 mL (1g/L) to each sample. The results are shown in Fig. 5 and show a decrease in photodegradation activity with increasing TCP concentration, related to the insufficient amount of $HO^{\cdot}$ radicals to degrade all the organic molecules present in the solution. The TCP concentration (0.5 mM) has a high removal efficiency compared to 0.7 and 1 mM, reaching 96%, 90% and 40%, respectively, at 200 min (Fig. 5). This is due to the availability of sufficient catalyst surface area and low intermediate production at this TCP concentration [71,72].

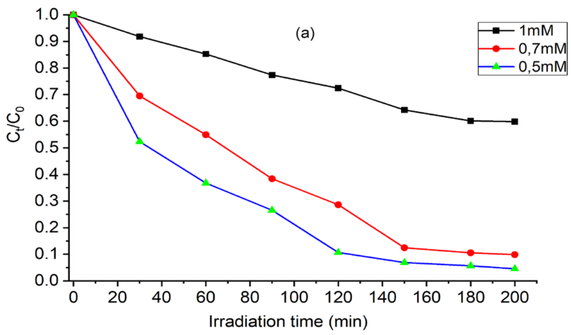

Fig. 5. Evolution of TCP concentration as a function of irradiation time (ratio: 1g TiO_2-LDH material/L of solution, pH=10)

In photocatalysis, the degradation is strongly influenced by the initial concentration, the process is favorable at low concentrations. The influence of the initial concentration is due to the following reasons: As the pollutant concentration increases, the amount of pollutant adsorbed on the outer surface of the catalyst increases, which causes its catalytic activity to decrease. Also, as the pollutant concentration increases, the path length of the photonic field passing through the solution decreases. Most of the hydroxyl radicals are consumed by secondary reactions before they can be effectively used for TCP removal. These results are in good agreement with those obtained by [69].

However, the abundant formation of intermediates at high TCP concentration at constant photocatalyst dose would compete with TCP molecules themselves on the photocatalytic surface, which explains the decrease in TCP degradation [73]. Therefore, the optimal concentration of TCP is 0.5 mM. However, the concentration of 1 mM was chosen to evaluate the maximum reaction rate.

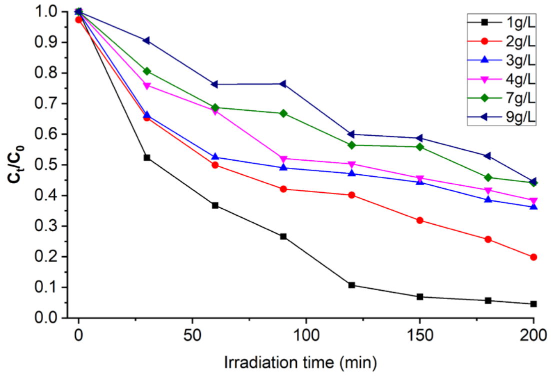

Fig. 6. Evolution of TiO_2-LDH concentration as a function of irradiation time (1-9g TiO_2-LDH/L of solution, C (TCP)=0.5mM, pH=10).

According to the literature [20,63], the degradation of TCP produces by-products such as 2,6-dichlorophenol, 2,4-dichlorophenol, 4-chlorophenol, hydroquinone, phenol, benzoquinone and others [72]. The resulting organic radicals then react with oxygen to initiate a series of degrading oxidation reactions that eventually lead to mineralization products such as CO_2 and H_2O by opening the aromatic cycle during the photocatalytic process [74,75].

In order to study the effect of the mass of TiO_2-LDH on the photodegradation of TCP, several masses ranging from 0.1 to 0.9 g were added to each sample of a solution with a concentration of 0.5 mM TCP in a volume of 100 mL, and irradiated for 0-200 min. The results are shown in the Fig. 6, showing a remarkable increase in photodegradation efficiency with decreasing mass of TiO_2-LDH, reaching maximum values of 95.4%, 80.1%, 63.8%, 61.6%, 55.8% and 55.4% at 1, 2, 3, 4, 7 and 9 g/L TiO_2-LDH, respectively.

4. Conclusions

In this work, a TiO_2/LDH nanocomposite was synthesized by co-precipitation. Its catalytic performance towards a TCP phenolic compound has been studied. The material was prepared under different physico-chemical parameters (pH, concentration, ratio of the mass of the nanocomposite to the volume of the solution), in order to identify the optimal preparation conditions and maximize the degradation efficiency of TCP. Structural analysis showed that the addition of TiO_2 in LDH matrices induces profound changes in the textural properties of the solid, increasing the surface area and pore volume. The results also showed that the conversion rate is directly affected by the pH.

Better photodegradation is achieved at basic pH, because the acidic medium alters the structure of the LDHs. In photocatalysis, the degradation is strongly influenced by the initial concentration of the pollutant. The process is favorable at low concentrations because the amount of $HO^{\bullet}$ radicals of the nanocomposite is not sufficient to degrade all the organic molecules present in the solution. Therefore, TCP (0.5mM) has a higher removal efficiency compared to 0.7 and 1mM, reaching up to 96% of degradation. In this environmentally friendly form, TiO_2, which is well immobilized on the clay, poses no risk. In addition, TiO_2/LDH nanocomposites are considered to be inexpensive and easily recyclable materials.

Acknowledgments

This work is the result of a close collaboration between the two laboratories LPCMCE of the USTOMB and UMET of the University of Lille, within the framework of a research program of Hubert Curien Tassili (PHC). Our thanks therefore go first of all to the various actors involved in the implementation of this project. The authors are grateful for the support of the Algerian Ministry of Higher Education and Scientific Research (MESRS), the General Directorate of Scientific Research and Technological Development (DGRSDT) of Algeria, the University of Science and Technologies of Oran/Algeria, the CNRS, and the University of Lille/France.

REFERENCES

[1]. *S. Garcia-Segura, E. Brillas*, Applied photoelectrocatalysis on the degradation of organic pollutants in wastewaters, Journal of Photochemistry and Photobiology C: Photochemistry Reviews, **vol. 31**, 2017, pp. 1–35

[2]. *F.J. Benitez, J. Beltran-Heredia, J.L. Acero, F.J. Rubio*, Contribution of free radicals to chlorophenols decomposition by several advanced oxidation processes, Chemosphere, **vol. 41**, 2000, pp. 1271–1277

[3]. *S.R. Hernandez, S.V. Kergaravat, M.I. Pividori*, Enzymatic electrochemical detection coupled to multivariate calibration for the determination of phenolic compounds in environmental samples, Talanta, **vol. 106**, 2013, pp. 399–407

[4]. *A. Karci, I. Arslan-Alaton, T. Olmez-Hanci, M. Bekbölet,* Transformation of 2,4-dichlorophenol by H_2O_2/UV-C, Fenton and photo-Fenton processes: Oxidation products and toxicity evolution. Journal of Photochemistry and Photobiology A: Chemistry, **vol. 230**, 2012, pp. 65–73

[5]. *D. Liu, Z. Huang, M. Li, et al.,* Construction of magnetic bifunctional β-cyclodextrin nanocomposites for adsorption and degradation of persistent organic pollutants, Carbohydrate Polymers, **vol. 230**, 2020, pp. 115564

[6]. *P. Singh, A. Borthakur,* A review on biodegradation and photocatalytic degradation of organic pollutants: A bibliometric and comparative analysis, Journal of Cleaner Production, **vol. 196**, 2018, pp. 1669–1680

[7]. *F. Ghanbari, M. Moradi,* Application of peroxymonosulfate and its activation methods for degradation of environmental organic pollutants: Review, Chemical Engineering Journal, **vol. 310**, 2017, pp. 41–62

[8]. *M.H. Rasoulifard, S.M.M. Doust Mohammadi, A. Heidari, G.H. Shahverdizadeh,* Photocatalytic degradation of acid red 14 from contaminated water using immobilized TiO_2 nanoparticles on glass beads activated by UV/peroxydisulfate, Desalination and Water Treatment, **vol. 52**, 2014, pp. 5479–5484

[9]. *R. Goslich, R. Dillert, D. Bahnemann,* Solar water treatment: principles and reactors, Water Science and Technology, **vol. 35**, 1997, pp. 137–148

[10]. *S. Chala, K. Wetchakun, S. Phanichphant, et al.,* Enhanced visible-light-response photocatalytic degradation of methylene blue on Fe-loaded $BiVO_4$ photocatalyst, Journal of Alloys and Compounds, **vol. 597**, 2014, pp. 29–135

[11]. *L.M. Bellotindos, A.T. Chang, M.C. Lu,* Degradation of acetaminophen by different Fenton processes, Desalination and Water Treatment, **vol. 56**, 2015, pp. 1372–1378

[12]. *W. Li, Q. Zhou, T. Hu,* Removal of organic matter from landfill leachate by advanced oxidation processes: A review, International Journal of Chemical Engineering, **vol. 2010**, 2010, pp. 270532

[13]. *L. Bruner, J. Kozak,* Information on the photocatalysis I the light reaction in uranium salt plus oxalic acid mixtures, Z. Elektrochem. Angew. Phys. Chem., **vol. 17**, 1911, pp. 354–360

[14]. *N Serpone, A.V. Emeline, S. Horikoshi, et al.,* On the genesis of heterogeneous photocatalysis: a brief historical perspective in the period 1910 to the mid-1980s, Photochemical & Photobiological Sciences, **vol. 11**, 2012, pp. 1121–1150

[15]. *O. Autin, J. Hart, P. Jarvis, et al.,* The impact of background organic matter and alkalinity on the degradation of the pesticide metaldehyde by two advanced oxidation processes: UV/H_2O_2 and UV/TiO_2, Water Research, **vol. 47**, 2013, pp. 2041–2049

[16]. *S.M. Miron, J. Brendlé, L. Josien, et al.,* Development of a new cathode for the electro-Fenton process combining carbon felt and iron-containing organic–inorganic hybrids, Comptes Rendus Chimie, **vol. 22**, 2019, pp. 238–249

[17]. *M. Sillanpää, M.C. Ncibi, A. Matilainen, M. Vepsäläinen,* Removal of natural organic matter in drinking water treatment by coagulation: A comprehensive review, Chemosphere, **vol. 190**, 2018, pp. 54–71

[18]. *M. Yasmina, K. Mourad, S.H. Mohammed, C. Khaoula,* Treatment Heterogeneous Photocatalysis; Factors Influencing the Photocatalytic Degradation by TiO_2, Energy Procedia, **vol. 50**, 2014, pp. 559–566

[19]. *L. Popescu, D. Creanga, L. Sacarescu, M. Grigoras, N. Lupu,* Magnetic nanoparticles for Methylene Blue dye removal from wastewater, UPB Scientific Bulletin, Series A: Applied Mathematics and Physics, **vol. 81**, 2019, pp. 241-252

[20]. *U.I. Gaya, A.H. Abdullah, M.Z. Hussein, Z. Zainal,* Photocatalytic removal of 2,4,6-trichlorophenol from water exploiting commercial ZnO powder, Desalination, **vol. 263**, 2010, pp. 176–182

[21]. *X. Ma, Y. Dai, M. Guo, B. Huang,* Insights into the role of surface distortion in promoting the separation and transfer of photogenerated carriers in anatase TiO_2, Journal of Physical Chemistry C, **vol. 117**, 2013, pp. 24496–24502

[22]. *X. Ma, Y. Dai, B. Huang,* Origin of the increased photocatalytic performance of TiO_2 nanocrystal composed of pure core and heavily nitrogen-doped shell: A theoretical study, ACS Applied Materials and Interfaces, **vol. 6**, 2014, pp. 22815–22822

[23]. *C. Ooka, H. Yoshida, M. Horio, et al.,* Adsorptive and photocatalytic performance of TiO_2 pillared montmorillonite in degradation of endocrine disruptors having different hydrophobicity, Applied Catalysis B: Environmental, **vol. 41**, 2003, pp. 313–321

[24]. *S. Miao, Z. Liu, B. Han, et al.,* Synthesis and characterization of TiO_2-montmorillonite nanocomposites and their application for removal of methylene blue, Journal of Materials Chemistry, **vol. 16**, 2006, pp. 579-584

[25]. *W.H. Zhang, X.D. Guo, J. He, Z.Y. Qian,* Preparation of Ni(II)/Ti(IV) layered double hydroxide at high supersaturation, Journal of the European Ceramic Society, **vol. 28**, 2008, pp. 1623–1629

[26]. *R.J. Tayade, R.G. Kulkarni, R.V. Jasra,* Enhanced Photocatalytic Activity of TiO_2-Coated NaY and HY Zeolites for the Degradation of Methylene Blue in Water, Industrial and Engineering Chemistry Research, **vol. 46**, 2006, pp. 369–376

[27]. *M. Takeuchi, T. Kimura, M. Hidaka, et al.,* Photocatalytic oxidation of acetaldehyde with oxygen on TiO_2/ZSM-5 photocatalysts: Effect of hydrophobicity of zeolites, Journal of Catalysis, **vol. 246**, 2007, pp. 235–240

[28]. *M. Takeuchi, J. Deguchi, M. Hidaka, et al.,* Enhancement of the photocatalytic reactivity of TiO_2 nano-particles by a simple mechanical blending with hydrophobic mordenite (MOR) zeolite, Applied Catalysis B: Environmental, **vol. 89**, 2009, pp. 406–410

[29]. *R. Sellappan, A. Galeckas, V. Venkatachalapathy, et al.,* On the mechanism of enhanced photocatalytic activity of composite TiO_2/carbon nanofilms. Applied Catalysis B: Environmental, **vol. 106**, 2011, pp. 337–342

[30]. *M.J. Sampaio, C.G. Silva, R.R.N. Marques, et al.,* Carbon nanotube–TiO_2 thin films for photocatalytic applications, Catalysis Today, **vol. 161**, 2011, pp. 91–96

[31]. *Y. Yao, F. Xu, M. Chen, et al.,* Adsorption behavior of methylene blue on carbon nanotubes, Bioresource Technology, **vol. 101**, 2010, pp. 3040–3046

[32]. *T. An, J. Chen, G. Li, et al.,* Characterization and the photocatalytic activity of TiO_2 immobilized hydrophobic montmorillonite photocatalysts: Degradation of decabromodiphenyl ether (BDE 209), Catalysis Today, **vol. 139**, 2008, pp. 69–76

[33]. *C. Gómez-Solís, I. Juárez-Ramírez, E. Moctezuma, L.M. Torres-Martínez,* Photodegradation of indigo carmine and methylene blue dyes in aqueous solution by SiC–TiO_2 catalysts prepared by sol–gel, Journal of Hazardous Materials, **vol. 217–218**, 2012, pp. 194–199

[34]. *Z. Huang, P. Wu, Y. Lu, et al.,* Enhancement of photocatalytic degradation of dimethyl phthalate with nano-TiO_2 immobilized onto hydrophobic layered double hydroxides: A mechanism study, Journal of Hazardous Materials, **vol. 246–247**, 2013, pp. 70–78

[35]. *E.L. Crepaldi, P.C. Pavan, J.B. Valim,* Comparative study of the coprecipitation methods for the preparation of Layered Double Hydroxides, Journal of the Brazilian Chemical Society, **vol. 11**, 2000, pp. 64–70

[36]. *U. Costantino, F. Marmottini, M. Nocchetti, R. Vivani,* New Synthetic Routes to Hydrotalcite-Like Compounds - Characterisation and Properties of the Obtained Materials, European Journal of Inorganic Chemistry, **vol. 1998**, 1998, pp. 1439-1446

[37]. *N. Iyi, H. Yamada, T. Sasaki,* Deintercalation of carbonate ions from carbonate-type layered double hydroxides (LDHs) using acid–alcohol mixed solutions, Applied Clay Science, **vol. 54**, 2011, pp. 132–137

[38]. *J. Rocha, M. Del Arco, V. Rives, M.A. Ulibarri,* Reconstruction of layered double hydroxides from calcined precursors: a powder XRD and ^{27}Al MAS NMR study, Journal of Materials Chemistry, **vol. 9**, 1999, pp. 2499–2503

[39]. *T. Stanimirova, V. Balek,* Characterization of layered double hydroxide Mg-Al-CO_3 prepared by re-hydration of Mg-Al mixed oxide, Journal of Thermal Analysis and Calorimetry, **vol. 94**, 2008, pp. 477–481

[40]. *S. Aisawa, S. Takahashi, W. Ogasawara, et al.,* Direct Intercalation of Amino Acids into Layered Double Hydroxides by Coprecipitation, Journal of Solid State Chemistry, **vol. 162**, 2001, pp. 52–62

[41]. *T. Ge, J. Han, Y. Qi, et al.,* The toxic effects of chlorophenols and associated mechanisms in fish, Aquatic Toxicology, **vol. 184**, 2017, pp. 78–93

[42]. *C.G. Joseph, G.L. Puma, A. Bono, et al.,* Operating parameters and synergistic effects of combining ultrasound and ultraviolet irradiation in the degradation of 2,4,6-trichlorophenol, Desalination, **vol. 276**, 2011, pp. 303–309
[43]. *C. Schummer, M. Sadiki, P. Mirabel, M. Millet,* Analysis of t-butyldimethylsilyl derivatives of chlorophenols in the atmosphere of urban and rural areas in East of France, Chromatographia, **vol. 63**, 2006, pp. 189–195
[44]. *N.K. Temel, M. Sökmen,* New catalyst systems for the degradation of chlorophenols, Desalination, **vol. 281**, 2011, pp. 209–214
[45]. *S. Chaliha, K.G. Bhattacharyya,* Catalytic wet oxidation of 2-chlorophenol, 2,4-dichlorophenol and 2,4,6-trichlorophenol in water with Mn(II)-MCM41, Chemical Engineering Journal, **vol. 139**, 2008, pp. 575–588
[46]. *Y. Jiang, C. Petrier, T.D. Waite,* Sonolysis of 4-chlorophenol in aqueous solution: Effects of substrate concentration, aqueous temperature and ultrasonic frequency, Ultrasonics Sonochemistry, **vol. 13**, 2006, pp. 415–422
[47]. *P. Gharbani, A. Mehrizad,* Heterogeneous catalytic ozonation process for removal of 4-chloro-2-nitrophenol from aqueous solutions, Journal of Saudi Chemical Society, **vol. 18**, 2014, pp. 601–605
[48]. *H. Bashiri, M. Rafiee,* Kinetic Monte Carlo simulation of 2,4,6-thrichlorophenol ozonation in the presence of ZnO nanocatalyst, Journal of Saudi Chemical Society, **vol. 20**, 2016, pp. 474–479
[49]. *A. Simon, C. Ballai, G. Lente, I. Fábián,* Structure–reactivity relationships and substituent effect additivity in the aqueous oxidation of chlorophenols by cerium(IV), New Journal of Chemistry, **vol. 35**, 2011, pp. 235–241
[50]. *N. Graham, W. Chu, C. Lau,* Observations of 2,4,6-trichlorophenol degradation by ozone, Chemosphere, **vol. 51**, 2003, pp. 237–243
[51]. *K. Yoshida, T. Shigeoka, F. Yamauchi,* Evaluation of aquatic environmental fate of 2,4,6-trichlorophenol with a mathematical model, Chemosphere, **vol. 16**, 1987, pp. 2531–2544
[52]. *P. Klug, L.E. Alexander,* X-Ray diffraction procedures, Wiley, New York, 1974
[53]. *L. Stoica, F. Bygrave, J. Andrew,* Barium titanate thin films for novel memory applications, UPB Scientific Bulletin, Series A: Applied Mathematics and Physics, **vol. 75**, 2013, pp. 147-158
[54]. *C. Catalin Armeanu,* 3D X-ray image composition, UPB Scientific Bulletin, Series A: Applied Mathematics and Physics, **vol. 78**, 2016, pp. 309-320
[55]. *L.-A. Nita, M. Iovea, G. Suliman, A. Enciu, M. Neagu,* Preliminary tests for speckle-based x-ray phase-contrast imaging: Optimization, UPB Scientific Bulletin, Series A: Applied Mathematics and Physics, **vol. 85**, 2023, pp. 149-158
[56]. *J. Kauppinen, J. Partanen,* Fourier transforms in spectroscopy, John Wiley & Sons, Berlin, Germany, 2001
[57]. *A. Dutta,* Chapter 4 - Fourier Transform Infrared Spectroscopy, Editors: S. Thomas, R. Thomas, A.K. Zachariah, R.K. Mishra, In Micro and Nano Technologies, Spectroscopic Methods for Nanomaterials Characterization, Elsevier, 2017, pp. 73-93
[58]. *M. Frenți, C. Mița, N. Cornei, V. Tiron, G. Bulai, M. Dobromir, A. Doroshkevich, D. Mardare,* ZrO_2 for photocatalytic applications, UPB Scientific Bulletin, Series A: Applied Mathematics and Physics, **vol. 85**, 2023, pp. 165-176
[59]. *L. Ivanjek, P.S. Shaffer, L.C. McDermott, M. Planinic, D. Veza,* Research as a guide for curriculum development: An example from introductory spectroscopy. II. Addressing student difficulties with atomic emission spectra, American Journal of Physics, **vol. 83**, 2015, pp.171-178

[60]. *I.V. Popescu, C. Stihi, G.V. Cimpoca, G. Dima, G. Vlaicu, A. Gheboianu, I. Bancuta, V. Ghisa, G. State,* Environmental Samples Analysis by Atomic Absorption Spectrometry (AAS) and Inductively Coupled Plasma-Optical Emission Spectroscopy (ICP-AES), Romanian Journal of Physics, **vol. 54**, 2009, pp.731-741

[61]. *R. Selvaraju, R.G. Raman, R. Narayanaswamy, R. Valliappan, R. Baskaran,* Trace element analysis in hepatitis B affected human blood serum by inductively coupled plasma-atomic emission spectroscopy (ICP-AES), Romanian Journal of Biophysics, **vol. 19**, 2009, pp.35-42

[62]. *F. Aoudjit, O. Cherifi, D. Halliche,* Simultaneously efficient adsorption and photocatalytic degradation of sodium dodecyl sulfate surfactant by one-pot synthesized TiO_2/layered double hydroxide materials, Separation Science and Technology, **vol. 54**, 2019, pp. 1095–1105

[63]. *T.V. Toledo, C.R. Bellato, R.H. do Rosário, J. de Oliveira Marques Neto,* Adsorption of arsenic(V) by the magnetic hydrotalcite: iron oxide composite, Química Nova, **vol. 34**, 2011, pp. 561–567

[64]. *T.V. Toledo, C.R. Bellato, K.D. Pessoa, M.P. Ferreira,* Removal of chromium (VI) from aqueous solutions using the calcined magnetic composite hydrotalcite-iron oxide: kinetic and thermodynamic equilibrium studies, Química Nova, **vol. 36**, 2013, pp. 419–425

[65]. *M. Bouraada, M. Lafjah, M.S. Ouali, L.C. de Menorval,* Basic dye removal from aqueous solutions by dodecylsulfate- and dodecyl benzene sulfonate-intercalated hydrotalcite. Journal of Hazardous Materials, **vol. 153**, 2008, pp. 911–918.

[66]. *M. Zhao, Z. Tang, P. Liu,* Removal of methylene blue from aqueous solution with silica nano-sheets derived from vermiculite, Journal of Hazardous Materials, **vol. 158**, 2008, pp. 43–51

[67]. *M.F. De Almeida, C.R. Bellato, A.H. Mounteer, et al.,* Enhanced photocatalytic activity of TiO_2-impregnated with MgZnAl mixed oxides obtained from layered double hydroxides for phenol degradation, Applied Surface Science, **vol. 357**, 2015, pp. 1765–1775

[68]. *A. Vaccari,* Layered double hydroxides: present and future, 1st. Nova Science Publishers, Inc., New York, USA, 2001.

[69]. *P. Saritha, D.S.S. Raj, C. Aparna, et al.*, Degradative oxidation of 2,4,6 trichlorophenol using advanced oxidation processes - A comparative study, Water, Air, and Soil Pollution, **vol. 200**, 2009, pp. 169–179

[70]. *M.H.H. Ali, K.M. Al-Qahtani, S.M. El-Sayed,* Enhancing photodegradation of 2,4,6 trichlorophenol and organic pollutants in industrial effluents using nanocomposite of TiO_2 doped with reduced graphene oxide, Egyptian Journal of Aquatic Research, **vol. 45**, 2019, pp. 321–328

[71]. *S. Ahmed, M.G. Rasul, W.N. Martens, et al.,* Heterogeneous photocatalytic degradation of phenols in wastewater: A review on current status and developments, Desalination, **vol. 261**, 2010, pp. 3–18

[72]. *A. Zada, M. Khan, M.A. Khan, et al.,* Review on the hazardous applications and photodegradation mechanisms of chlorophenols over different photocatalysts, Environmental Research, **vol. 195**, 2021, pp. 110742

[73]. *N. Kashif, F. Ouyang,* Parameters effect on heterogeneous photocatalysed degradation of phenol in aqueous dispersion of TiO_2, Journal of Environmental Sciences, **vol. 21**, 2009, pp. 527–533

[74]. *O. Legrini, E. Oliveros, A.M. Braun,* Photochemical Processes for Water Treatment, Chemical Reviews, **vol. 93**, 1993, pp. 671–698

[75]. *R.J. Kieber, G.R. Helz,* Two-Method Verification of Hydrogen Peroxide Determinations in Natural Waters, Analytical Chemistry, **vol. 58**, 1986, pp. 2312–2315